Phys. Status Solidi RRL **8**, No. 5, 381–384 (2014) / **DOI** 10.1002/pssr.201409143

The BOSCO solar cell – a both sides collecting and contacted structure

Fabian Fertig*, Karin Krauß, Johannes Greulich, Florian Clement, Daniel Biro, Ralf Preu, and Stefan Rein

Fraunhofer ISE, Heidenhofstr. 2, 79110 Freiburg, Germany

Received 1 April 2014, revised 17 April 2014, accepted 17 April 2014
Published online 28 April 2014

Keywords multicrystalline silicon, bifacial structures, double-sided collection, solar cells

* Corresponding author: e-mail fabian.fertig@ise.fraunhofer.de

The BOSCO solar cell represents a bifacial structure with double-sided collection. The structure allows the use of standard module interconnection technology and favours the use of material with low to medium diffusion length and low resistivity for maximum benefit towards other structures, such as Al-BSF and PERC. Within this work, we present first results on different multicrystalline silicon materials yielding a monofacial efficiency of 17.4% on large-area wafers from block-cast mc-Si. This value represents a gain of ~0.7%$_{abs}$ compared to Al-BSF cells processed in parallel. The applicability for bifacial operation is demonstrated by a significantly increased quantum efficiency for rear side illumination. These results make the BOSCO solar cell concept a promising candidate to further boost the output of utility-scale PV plants even when using low-cost wafers of low to medium diffusion length material.

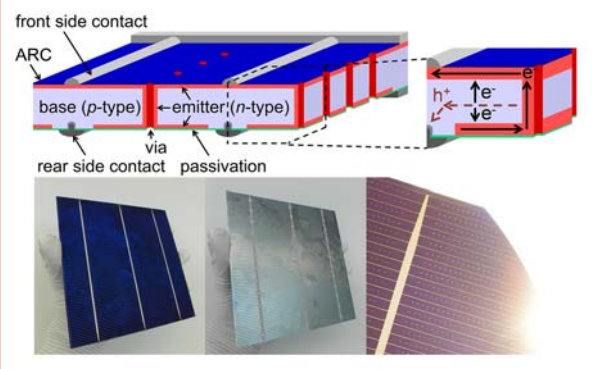

Sketch and photographs of the BOSCO solar cell concept.

1 Introduction In the past, several solar cell concepts [1–4] have aimed at utilizing the intrinsic advantage of architectures featuring a double-sided emitter in collection efficiency to overcome bulk diffusion length induced limitations of conversion efficiency. Although promising results have been achieved [5–7], the interest in such structures has cooled recently. Due to the rise of cell concepts featuring a grid on the rear side [8–12], bifacial applications have drawn increasing attention. However, published bifacial cell concepts generally require high bulk diffusion lengths and are, hence, preferably realized on n-type silicon substrates. The novel BOSCO ("*BO*th *S*ides *CO*llecting and *CO*ntacted") solar cell concept [13] is beneficial for substrates with low diffusion length *and* favours bifacial application. Within this work we show first experimental results on large-area multicrystalline silicon (mc-Si) wafers.

2 The cell concept The BOSCO solar cell architecture is sketched in the abstract figure. Front and rear side areas are interconnected by diffused vias and the rear-side emitter area is disconnected from the base contact. The cell concept features a contact grid on both sides and the front and rear side busbars run in parallel. This allows the use of standard module interconnection technology. The photographs of a multicrystalline silicon BOSCO solar cell shown in the abstract figure illustrate the symmetric grid layout applied. If a transparent module backsheet or a glass/glass module composition is applied, the bifacial nature of the BOSCO solar cell concept can be fully utilized.

As illustrated in the sketch above, the minority carriers generated in the base can be collected on both sides in the double-sided emitter regions. This effect leads to increased collection efficiency and recombination in the base [2, 14].

Hence, a higher short-circuit current density J_{sc} compared to single-sided collecting structures is expected and when bulk recombination is the dominant recombination mechanism, a lower open-circuit voltage V_{oc}. For low bulk recombination, the recombination at the rear side determines V_{oc}, again in comparison to single-sided collecting structures. To reach the external contacts, majority carries have to drift laterally in the base (holes) and, partly, from the rear side emitter through the vias and the front side emitter (electrons). This lateral drift of the majority carriers causes fill factor *FF* losses due to series resistance and non-generation losses [2, 14, 15]. In order to quantify these effects on conversion efficiency, two-dimensional numerical device simulations have been performed with Sentaurus TCAD [16]. For carrier mobilities, Schindler's extension [17] of Klaassen's model [18, 19] is applied and all other models are chosen as summarized in Ref. [20]. The generation profile is assumed the same for aluminium back surface field (Al-BSF) and BOSCO solar cells to focus on cell concept specific differences in the electric parameters. For the doped regions, dark saturation current densities of $j_{0e,front} = 150$ fA/cm^2 and $j_{0e,rear} = 100$ fA/cm^2 are assumed for the emitters on the textured front and the planar rear side, respectively, and $j_{0,bsf} = 300$ fA/cm^2 for the Al-BSF.

Figure 1c shows simulation results for the difference in monofacial conversion efficiency between the BOSCO and Al-BSF cell concept depending on base resistivity ρ_b and bulk diffusion length L_{bulk}. For $\rho_b < 1.5$ Ω cm, the increase in J_{sc} overcompensates the limitation in *FF*. Figure 1b shows a cut of Fig. 1c at $\rho_b = 0.5$ Ω cm and Fig. 1a absolute values for maximum output power density p_{MPP}. In addition to monofacial illumination, a bifacial scenario assuming a rear side illumination intensity of $E_{rear} = 0.1$ suns is considered. A significant gain is achieved, also for low bulk diffusion lengths. The discussed advantages of the BOSCO cell concept become even more pronounced when assuming dopant compensation in the base (not shown). These results strongly motivate the application of the BOSCO solar cell concept to material with low base resistivity and low to medium diffusion length.

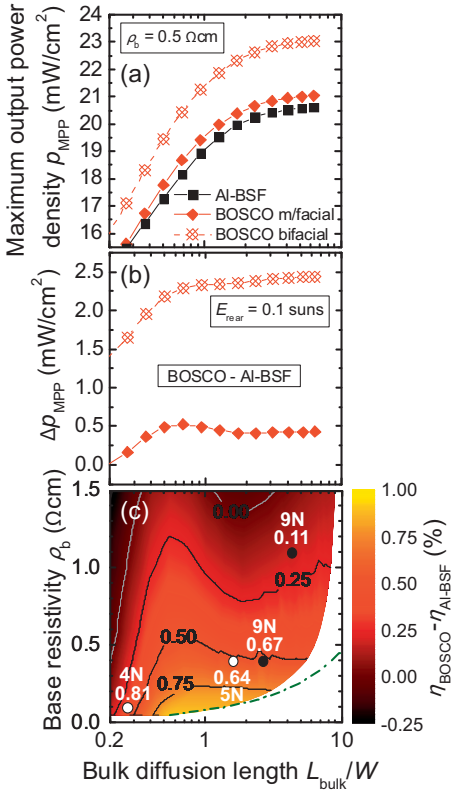

Figure 1 Results of two-dimensional numerical simulations. (a) Maximum output power density p_{MPP} of the BOSCO and Al-BSF cell concepts and (b) difference of BOSCO to Al-BSF cell for mono- and bifacial illumination. (c) Difference in monofacial conversion efficiency between BOSCO and Al-BSF cell concepts. The green dash-dotted curve indicates the Auger limit in low level injection according to Richter et al. [21]. A cell thickness of $W = 180$ µm is assumed. Open symbols represent experimentally gained values for UMG and closed symbols for EG mc-Si.

3 Experimental results In order to evaluate the potential of the BOSCO cell concept experimentally, BOSCO cells were manufactured at Fraunhofer ISE on 15.6 × 15.6 cm^2 block-cast mc-Si wafers of varying purity and base resistivity. The investigated materials include upgraded metallurgical grade (UMG) silicon with a feedstock purity of 4N (i.e., 99.99% pure silicon) and 5N, as well as electronic-grade (EG) silicon with a purity of 9N. As a reference, Al-BSF cells were manufactured in parallel. The principle process flow of a BOSCO cell consists of the following steps:

- drilling of vias
- texture and optional rear side polish
- deposition of a structured diffusion barrier
- diffusion and PSG etch
- rear and front side passivation
- metallization

Hence, the process complexity is comparable to that of a passivated emitter and rear (PERC) cell [22].

Figure 2 and Table 1 show resulting illuminated *I*–*V* parameters for UMG and EG Si with $\rho_b = 0.4$ Ω cm measured on a non-reflecting chuck. That is, a potential gain due to transmitted and back-reflected illumination is excluded. As expected from the simulations, the increase in J_{sc} of +1.9 mA/cm^2 overcompensates the loss in *FF* of –2.5%$_{abs}$ to –2.6%$_{abs}$. The gain in J_{sc} is induced by better collection of long wavelength light due to the rear side emitter, see Fig. 3a. Along with a gain in V_{oc} of +9 mV to 10 mV, which is due to the less recombining rear side of the fabricated BOSCO cells, an efficiency gain of +0.6%$_{abs}$ to 0.7%$_{abs}$ could be demonstrated.

Figure 1c indicates the achieved experimental results in the simulated plot. A qualitatively good agreement can be observed with the BOSCO cells performing even somewhat better than predicted. This is due to better internal optics induced by the polished and dielectrically passivated

Table 1 Solar cell parameters of the two mc-Si material groups with $\rho_b \approx 0.4\ \Omega$ cm. Cell area is $A_{cell} = 15.6 \times 15.6\ cm^2$. All measurements were performed on a non-reflecting chuck.

feedstock purity	cell type	value (# cells)	V_{oc} (mV)	J_{sc} (mA/cm^2)	FF (%)	η (%)
UMG 5N	BOSCO	avg. (12)	636 ± 3	34.6 ± 0.2	76.6 ± 0.5	16.9 ± 0.1
UMG 5N		best*)	634	35.0	76.3	16.9
UMG 5N	Al-BSF	avg. (11)	626 ± 3	32.7 ± 0.5	79.2 ± 0.5	16.2 ± 0.3
UMG 5N		best*)	631	33.0	79.3	16.5
EG 9N	BOSCO	avg. (15)	632 ± 3	35.6 ± 0.1	77.0 ± 0.4	17.3 ± 0.2
EG 9N		best*)	634	35.4	77.4	17.4
EG 9N	Al-BSF	avg. (16)	622 ± 2	33.6 ± 0.3	79.5 ± 0.5	16.6 ± 0.2
EG 9N		best*)	629	33.7	79.8	16.9

*) Independently confirmed by Fraunhofer ISE Callab.

rear side of the manufactured BOSCO solar cells. The highest monofacial efficiency values independently confirmed by Fraunhofer ISE Callab are $\eta = 16.9\%$ for material UMG 5N and $\eta = 17.4\%$ for EG Si, compare Table 1.

In order to investigate the effect of the vias for double-sided collection and bifaciality, BOSCO cells with and without vias have been processed on neighbouring wafers. For the EG material, a gain in short-circuit current density of +0.9 mA/cm^2 due to the vias is reflected in a monofacial efficiency gain of +0.5%$_{abs}$, see Fig. 2. Figure 3b depicts internal quantum efficiencies of neighbouring cells with and without holes measured from the front and rear side, respectively, on a non-reflecting chuck. The vias allow higher carrier collection in the red wavelength regime when illuminated from the front side and, for rear side illumination, significantly higher collection across the entire wavelength range. It has to be noted that the cell without vias still collects additional current from the rear side emitter across the edges leading to double-sided collection being not switched off completely. This also leads to an increase in monofacial J_{sc}, see Fig. 2b. A cell with a front-side emitter only would exhibit an even lower IQE from either side. Hence, Fig. 3b illustrates that the BOSCO solar cell concept allows for significant carrier collection for rear side illumination even when using low-diffusion-length material such as mc-Si.

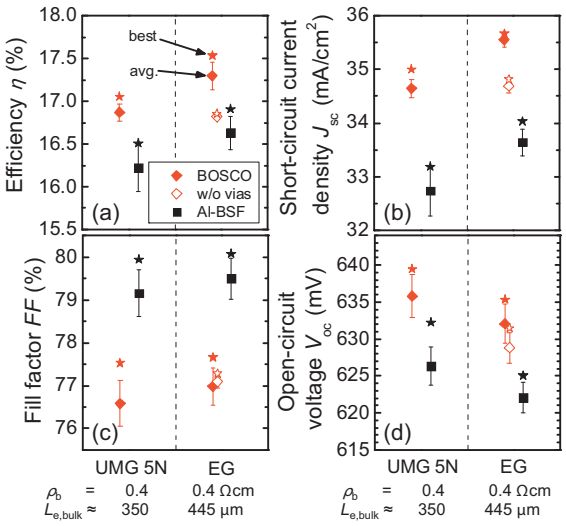

Figure 2 Illuminated I–V parameters: (a) η, (b) J_{sc}, (c) FF and (d) V_{oc} for large-area mc-Si cells from UMG and EG feedstock measured on a non-reflecting chuck.

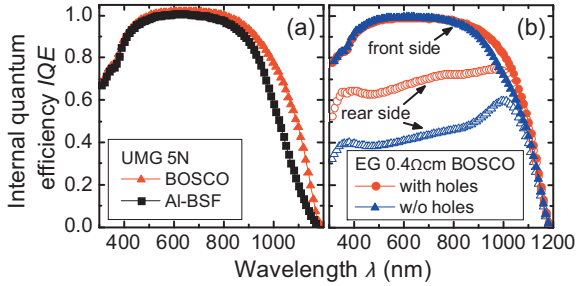

Figure 3 Internal quantum efficiencies on neighbouring wafers of (a) Si material 'UMG 5N' for BOSCO and Al-BSF cells and (b) material 'EG' for BOSCO cells with and without vias measured from the front and rear side on a non-reflecting chuck.

4 Conclusion By means of simulation and experiment, we have shown that the BOSCO cell concept is a promising candidate to enable bifacial applications for low to medium diffusion length material such as multicrystalline silicon due to its double-sided emitter. A significant gain in monofacial efficiency of +0.7%$_{abs}$ compared to Al-BSF cells has been achieved on different mc-Si materials. A significantly increased quantum efficiency for rear side illumination demonstrates the possible application of bifacial module concepts for low-diffusion-length material. Since the BOSCO cell concept features a standard busbar layout, standard module interconnection technology can be applied for industrial production.

Acknowledgements This work has been supported by the Fraunhofer Society within the project SiliconBeacon. K. Krauß

gratefully acknowledges the scholarship of the German Federal Environmental Foundation ("Deutsche Bundesstiftung Umwelt").

References

[1] J. M. Gee, W. K. Schubert, and P. A. Basore, in: Record of the 23rd IEEE Photovoltaic Specialists Conference, Louisville, KY, USA, 1993, pp. 265–270.
[2] A. Luque, A. Cuevas, and J. M. Ruiz, Solar Cells **2**, 151–166 (1980).
[3] I. Chambouleyron and Y. Chevalier, in: Proc. Photovoltaic Solar Energy Conference, Luxembourg, 1977, pp. 967–976.
[4] G. Willeke and P. Fath, in: Proc. 12th European Photovoltaic Solar Energy Conference, Amsterdam, Netherlands, 1994, pp. 766–768.
[5] ISFH, March 20th, 2012, press release.
[6] P. Engelhart, Lasermaterialbearbeitung als Schlüsseltechnologie zum Herstellen rückseitenkontaktierter Siliciumsolarzellen, Ph.D. thesis. Universität Hannover (2007).
[7] J. M. Gee and M. Wang, in: Proc. 26th European Photovoltaic Solar Energy Conference and Exhibition, Hamburg, Germany, 2011, pp. 1992–1995.
[8] A. R. Burgers et al., in: Proc. 26th European Photovoltaic Solar Energy Conference and Exhibition, Hamburg, Germany, 2011, pp. 1144–1147.
[9] S. de Wolf et al., Green **2**, 7–24 (2012).
[10] T. S. Böscke et al., IEEE J. Photovolt. **3**, 674–677 (2013).
[11] A. Edler et al., in: Proc. 28th European Photovoltaics Solar Energy Conference and Exhibition, Paris, France, 2013, pp. 967–970.
[12] S. Gall et al., in: Proc. 28th European Photovoltaics Solar Energy Conference and Exhibtion, Paris, France, 2013, pp. 695–698.
[13] F. Clement, Die Metal Wrap Through Solarzelle – Entwicklung und Charakterisierung, Ph.D. thesis, Albert-Ludwigs-Universität Freiburg (2009).
[14] J. Greulich et al., Energy Procedia **8**, 160–166 (2011).
[15] C. Ulzhöfer et al., J. Appl. Phys. **107**, 104509–104509 (2010).
[16] Sentaurus TCAD, "release H-2013.03" (2013).
[17] F. Schindler et al., Towards a unified model for carrier mobilities in crystalline silicon, submitted to Sol. Energy Mater. Sol. Cells (2014).
[18] D. Klaassen, Solid-State Electron. **35**, 953–959 (1992).
[19] D. Klaassen, Solid-State Electron. **35**, 961–967 (1992).
[20] P. P. Altermatt, J. Comput. Electron **10**, 314–330 (2011).
[21] A. Richter et al., Phys. Rev. B **86**, 165202 (2012).
[22] A. W. Blakers et al., Appl. Phys. Lett. **55**, 1363–1363 (1989).

